

## NON-ASSOCIATED SUPERELASTICITY IN ROTATING FRAME FORMULATION

BENOIT VIEILLE  
MOHAMMED LAMINE BOUBAKAR  
CHRISTIAN LEXCELLENT

*Laboratory of Applied Mechanics LMARC, Besancon, France  
e-mail: benoit.vieille01@edu.univ-fcomte.fr*

In order to describe and predict the superelastic finite strains behaviour of Shape Memory Alloys, a kinematic description with directors is proposed. Compatible with either isotropic or anisotropic behaviours, it allows a direct extension from the small perturbation formalism. Particularly, a general framework is proposed for the description of the Shape Memory Alloys superelastic behaviour under 3D proportional loadings.

*Key words:* Shape Memory Alloys, superelasticity, finite strains, normality rule, non-associated constitutive framework

### Notations

Tensors will be denoted by bold letters. Their juxtaposition implies the usual double contraction operation. Superposed  $S$  and  $A$  indicate respectively a symmetric tensor  $(\bullet)^S$  and an antisymmetric tensor  $(\bullet)^A$ . A superposed dot  $\dot{(\bullet)}$  indicates the usual time derivative.  $\partial_X(\bullet)$  denotes the partial derivative of  $(\bullet)$  with respect to  $X$ .  $\mathbf{I}$  is the second order identity tensor. Finally,  $\|\bullet\|$  is the Euclidean norm.

## 1. Introduction

Among the different materials considered to be smart, i.e. adapting themselves to their environment, the Shape Memory Alloys do present interesting properties, namely the shape memory effect and the superelasticity. Those properties rest on a phase transformation: the martensitic transformation, from a

parent phase called austenite to a product phase called martensite, occurring in the material subjected to a stress and/or temperature. Superelasticity is certainly one of the most studied properties of that kind of material. Up to now, many SMA constitutive models in 1D have been developed in the past few years for structural elements such as wires, rods and beams. However, very few 3D models have been studied to represent the behaviour of SMA in 3D structures.

The present work aims at modelling the SMA finite strains superelasticity behaviour thanks to a rotating frame formulation. This one is based on the director vectors concept presented in the following part. Within this approach, the transformation gradient decomposition allows to get the partition of a cumulated tensorial deformation in a formalism close to the small perturbations one. Using the notion of "constrained equilibrium", the thermodynamic description is based, like in the small strains hypothesis, on an assumed non-convex specific free energy function and two independent normal dissipative processes, i.e. one for the forward transformation, the other for the reverse transformation. The evolution laws of both transformations are derived from a suitable maximum dissipation principle. The consequent constitutive equations can be time-discretized thanks to a method based on the forward Euler time discretization (explicit integration) and then implemented in a finite element code.

## 2. Finite transformations kinematics

The approach used to build a finite transformations kinematics for the SMA thermomechanical behaviour study is based on the concept of the deformed intermediate configuration introduced for the first time by Eckart (1948) and the notion of director vectors due to Cosserat and Cosserat (1909), resumed by Mandel (1971).

In the case of the SMA, the director vectors notion allows to orient and then to fix a non-relaxed intermediate configuration associated to the phase transition in the material. Assuming an elastic behaviour independent of the state phase, the following decomposition of the total transformation gradient is introduced

$$\mathbf{F} = (\mathbf{I} + \boldsymbol{\varepsilon}^e) \mathbf{q} \mathbf{F}^{tr} \quad (2.1)$$

$\mathbf{F}^{tr}$  is the transformation gradient due to the phase transition allowing to connect a reference configuration to an intermediate configuration in which a

director frame linked somehow to the material internal structure preserves its initial orientation. The evolution of this frame up to the current configuration, in which the elastic deformations  $\boldsymbol{\varepsilon}^e$  ( $\|\boldsymbol{\varepsilon}^e\| \ll 1$ ) are measured, is defined by rotation  $\mathbf{q}$  ( $\mathbf{q}^\top \mathbf{q} = \mathbf{I}$ ;  $\det \mathbf{q} = 1$ ).

The SMA are characterized by a possible reversible phase transition, austenite  $\leftrightarrow$  martensite. Their behaviour being associated with a solid-solid phase transition according to specific planes called habit planes, an orthonormal direct frame defined by these planes as an average of their orientation can be considered as the director (Fig. 1).

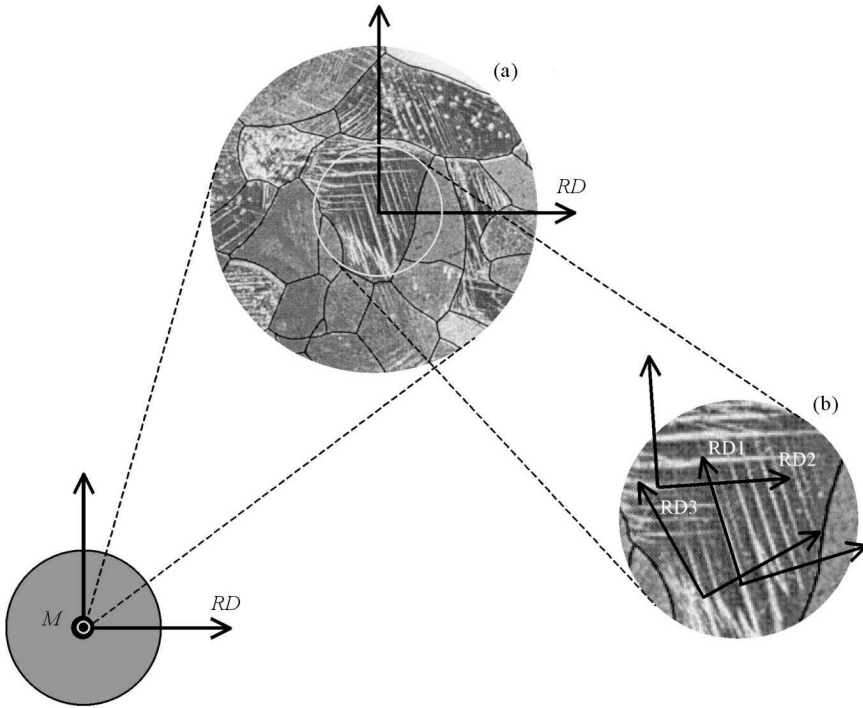


Fig. 1. Director frame (RD) for the Representative Volume Element (a) and the director frames linked to the habit planes (b)

The expression of the total transformation gradient (2.1) leads to the following decomposition of the material strain rate tensor  $\mathbf{D} = [\dot{\mathbf{F}}\mathbf{F}^{-1}]^S$  in the intermediate configuration

$$\mathbf{d}_q = \dot{\boldsymbol{\varepsilon}}_q^e + \mathbf{d}_q^{tr} \quad \mathbf{d}_q^{tr} = [\dot{\mathbf{F}}^{tr}(\mathbf{F}^{tr})^{-1}]^S \quad (2.2)$$

where

$$(\bullet)_q = \mathbf{q}^\top (\bullet) \mathbf{q}$$

and  $\mathbf{d}$  representing a cumulated tensorial deformation in the sense introduced in Gillormini *et al.* (1993).

The intermediate configuration can be defined by decomposition of the material spin  $\mathbf{W} = [\dot{\mathbf{F}}\mathbf{F}^{-1}]^A$  in the current configuration, by solving

$$\dot{\mathbf{q}} = (\mathbf{W} - \mathbf{W}^{tr})\mathbf{q} \quad \mathbf{q}\Big|_{t=0} = \mathbf{I} \quad \mathbf{W}^{tr} = \mathbf{q}\left[\dot{\mathbf{F}}^{tr}(\mathbf{F}^{tr})^{-1}\right]^A \mathbf{q}^\top \quad (2.3)$$

That is why the knowledge of the spin  $\mathbf{W}^{tr}$  of the material milieu, as regards its internal structure, is needed. Beyond the micro-macro approach seeming to be more natural to get this knowledge, the use of anti-symmetric isotropic tensorial functions representation theorems or the choice of a kinematic rotation consistent toward a phenomenological approach, are both other possibilities to assess the value of  $\mathbf{W}^{tr}$ . For random or pseudo-random distributions of the habit planes, a family of objective kinematics rotations  $\mathbf{q}$  can be defined by solving the following differential problem (Boubakar, 1994)

$$\dot{\mathbf{q}} = \left[(1 - \alpha)\mathbf{W} + \alpha\dot{\mathbf{R}}\mathbf{R}^\top\right]\mathbf{q} \quad \mathbf{q}\Big|_{t=0} = \mathbf{I} \quad \alpha \in ]0, 1] \quad (2.4)$$

where  $\mathbf{R}$  is the proper rotation associated with  $\mathbf{F}$ .

### 3. Constitutive frame in the intermediate configuration

The specific Helmholtz free energy for a three-dimensional formulation of the SMA behaviour is given by the following relation in the intermediate configuration, where  $\boldsymbol{\varepsilon}_q^e = \mathbf{d}_q - \mathbf{d}_q^{tr}$  (2.2) is the rotated elastic strain tensor from the current configuration,  $z$  is the martensite volume fraction and  $T$  is the temperature (Boubakar and LExcellent, 2002)

$$\psi = \psi(\boldsymbol{\varepsilon}_q^e, z, T) = \psi^{el}(\boldsymbol{\varepsilon}_q^e) + \psi^{ch-th}(z, T) + \psi^{di}(z, T) \quad (3.1)$$

$\psi^{di}(z, T)$  represents a specific coherency energy (Müller, 1989), and

$$\psi^{el}(\boldsymbol{\varepsilon}_q^e) = \frac{1}{2\rho}(\boldsymbol{\varepsilon}_q^e)^\top \mathbf{C}^e \boldsymbol{\varepsilon}_q^e \quad (3.2)$$

$$\psi^{ch-th}(z, T) = u_{0R}^a - T s_{0R}^a + C_v \left[ (T - T_R) - T \ln \frac{T}{T_R} \right] - z\pi_0(T)$$

$\pi_0(T) = (u_{0R}^a - u_{0R}^m) - T(s_{0R}^a - s_{0R}^m)$  is the driving force for temperature-induced phase transition at stress-free state ( $a$  representing the austenitic phase and

$m$  the martensitic phase),  $u_{0R}^a, u_{0R}^m, s_{0R}^a$  and  $s_{0R}^m$  being the values of internal energies and entropies at the chosen reference temperature  $T_R$ .

The fourth order elastic stiffness tensor  $\mathbf{C}^e$ , the specific heat  $C_v$  and the mass density  $\rho$  are assumed to be the same for both phases.

From the Clausius-Duhem inequality, the mechanical dissipation is then here

$$D^{mech} = (\dot{\mathbf{d}}_q^{tr})^\top \boldsymbol{\sigma}_q - R\dot{z} \geq 0 \qquad R = -\rho\pi_0(T) + \rho\partial_z\psi^{di}(z, T) \quad (3.3)$$

where  $\boldsymbol{\sigma}_q = \mathbf{q}^\top \boldsymbol{\sigma} \mathbf{q}$  is the rotated Cauchy stress tensor  $\boldsymbol{\sigma}$  of the current configuration. The forward transformation ( $a \rightarrow m$ ) is characterized by  $\dot{z} > 0$  and the reverse one ( $a \leftarrow m$ ) by  $\dot{z} < 0$ . Assuming a normal dissipative process for each transformation,  $D^{mech}$  can be defined by two independent dissipation functions of  $\dot{\mathbf{d}}_q^{tr}$  and  $\dot{z}$

$$D^{mech} = \begin{cases} D_{am}[\dot{\mathbf{d}}_q^{tr}, \dot{z}; (z, T)] & \text{if } \dot{z} > 0 \\ D_{ma}[\dot{\mathbf{d}}_q^{tr}, \dot{z}; (z, T)] & \text{if } \dot{z} < 0 \end{cases} \quad (3.4)$$

In the particular case of a time-independent behaviour (plasticity-like behaviour), these functions are convex, positively homogeneous of order one. Since the forward transformation ( $a \rightarrow m$ ) can be initiated in any loading direction,  $D_{am}$  is a quasi-positively homogeneous function defining a full convex cone in an eight-dimensional space such that  $D_{am}[(\mathbf{0}, 0); (z, T)] = 0$ . Following the generalized standard material theory (Halphen and Nguyen, 1975), the thermodynamic forces  $\boldsymbol{\sigma}_q$  and  $R$  belong then to the subdifferential  $\partial D_{am}$  of  $D_{am}$  and the dual variables  $\dot{\mathbf{d}}_q^{tr}$  and  $\dot{z}$  belong to the subdifferential  $\partial D_{am}^*$  of the indicator function of the convex domain  $\Omega_{am} = \{(\boldsymbol{\sigma}_q, R) / \varphi_{am}(\boldsymbol{\sigma}_q, R) \leq 0\}$ , i.e. the elasto-dissipative domain,  $\varphi_{am}$  defining a yield function. Thus

$$(\dot{\mathbf{d}}_q^{tr})^\top (\boldsymbol{\sigma}_q - \hat{\boldsymbol{\sigma}}_q) - (R - \hat{R})\dot{z} \geq 0 \qquad \forall [(\boldsymbol{\sigma}_q, \hat{\boldsymbol{\sigma}}_q), (R, \hat{R})] \in \Omega_{am} \quad (3.5)$$

what means that among all the admissible thermodynamic forces, the ones associated with a given set  $(\dot{\mathbf{d}}_q^{tr}, \dot{z})$  maximize the mechanical dissipation, i.e.

$$D^{mech} = \max_{(\hat{\boldsymbol{\sigma}}_q, \hat{R}) \in \Omega_{am}} \{(\dot{\mathbf{d}}_q^{tr})^\top \hat{\boldsymbol{\sigma}}_q - \hat{R}\dot{z}\} = \min_{(\hat{\boldsymbol{\sigma}}_q, \hat{R}) \in \Omega_{am}} \{-((\dot{\mathbf{d}}_q^{tr})^\top \hat{\boldsymbol{\sigma}}_q - \hat{R}\dot{z})\} \quad (3.6)$$

Considering the associated unconstrained minimization problem using the following Lagrange function

$$L_{am}(\hat{\boldsymbol{\sigma}}_q, \hat{R}, \dot{\lambda}_{am}) = -(\dot{\mathbf{d}}_q^{tr})^\top \hat{\boldsymbol{\sigma}}_q + \hat{R}\dot{z} + \dot{\lambda}_{am}\varphi_{am}(\hat{\boldsymbol{\sigma}}_q, \hat{R}) \quad (3.7)$$

the evolution laws giving  $\mathbf{d}_q^{tr}$  and  $\dot{z}$  for a forward transformation ( $a \rightarrow m$ ) are obtained classically from the  $L_{am}$  optimality conditions. In the standard Kuhn-Tucker form

$$\begin{aligned} \mathbf{d}_q^{tr} &= \dot{\lambda}_{am} \partial_{\sigma_q} \varphi_{am} & \dot{z} &= -\dot{\lambda}_{am} \partial_{\hat{R}} \varphi_{am} & \varphi_{am} &= 0 \\ \dot{\lambda}_{am} &\geq 0 & \dot{\lambda}_{am} \varphi_{am} &= 0 \end{aligned} \tag{3.8}$$

It can be stated from the yield condition  $\varphi_{am} = 0$  that  $\sigma_q = \hat{\sigma}_q$  and  $R = \hat{R}$ . The Lagrange multiplier  $\dot{\lambda}_{am}$  is derived from the consistency condition  $\dot{\varphi}_{am} = 0$ .

The normality assumption contained in these relations has been verified experimentally in Fig. 2 for CuAlBe alloys (Bouvet, 2001) where the arrows represent the phase transformation direction.

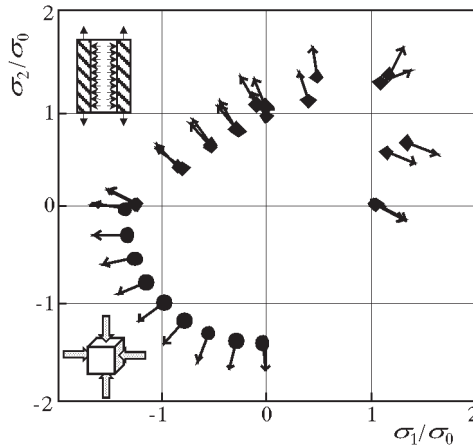


Fig. 2. Transformation outset surface in the case of bicompression and tension-internal pressure tests (Bouvet, 2001)

The following formal yield function can be introduced for the forward transformation

$$\varphi_{am}(\sigma_q, R) = \Sigma(\sigma_q) - \Sigma_{am}(R) \leq 0 \tag{3.9}$$

what leads to (Boubakar and Lexcellent, 2002)

$$\mathbf{d}_q^{tr} = \dot{\lambda}_{am} \partial_{\sigma_q} \Sigma \qquad \dot{z} = \dot{\lambda}_{am} \partial_R \Sigma_{am} = \frac{\dot{\lambda}_{am}}{\gamma_\Sigma} \tag{3.10}$$

Hence

$$\mathbf{d}_q^{tr} = \dot{z} \gamma_\Sigma \partial_{\sigma_q} \Sigma \tag{3.11}$$

$\gamma_\Sigma$  is the maximum phase transition strain in the direction of the threshold stress  $\Sigma_{am}$ . Following the definition of the elasto-dissipative domain  $\Omega_{am}$  in the thermodynamic forces space, the threshold stress  $\Sigma_{am}$  is defined as a function of  $R$ . However, from the expression of  $R$  in Eq. (3.3), it can be also considered as a constitutive function of  $z$  and  $T$  describing the effect of interaction between differently oriented crystals in the shape memory polycrystalline alloys. The scalar-valued function  $\Sigma$  of the rotated Cauchy stresses tensor or effective stress, is positively homogeneous of the first order and must verify  $\Sigma(\mathbf{Q}\boldsymbol{\sigma}_q^T\mathbf{Q}) = \Sigma(\boldsymbol{\sigma}_Q)$  for any rotation  $\mathbf{Q}$  of the intermediate configuration in the case of an isotropic behaviour. If the volumetric changes are negligible,  $\Sigma$  depends on the second and the third invariant of  $\boldsymbol{\sigma}_q$  (Boubakar *et al.*, 20020 in order to account for the superelasticity asymmetric character (Fig. 3). The invariants of  $\boldsymbol{\sigma}_q$  are also those of  $\boldsymbol{\sigma}$  since  $\boldsymbol{\sigma}_q$  is obtained from  $\boldsymbol{\sigma}$  thanks to an endomorphic transformation.

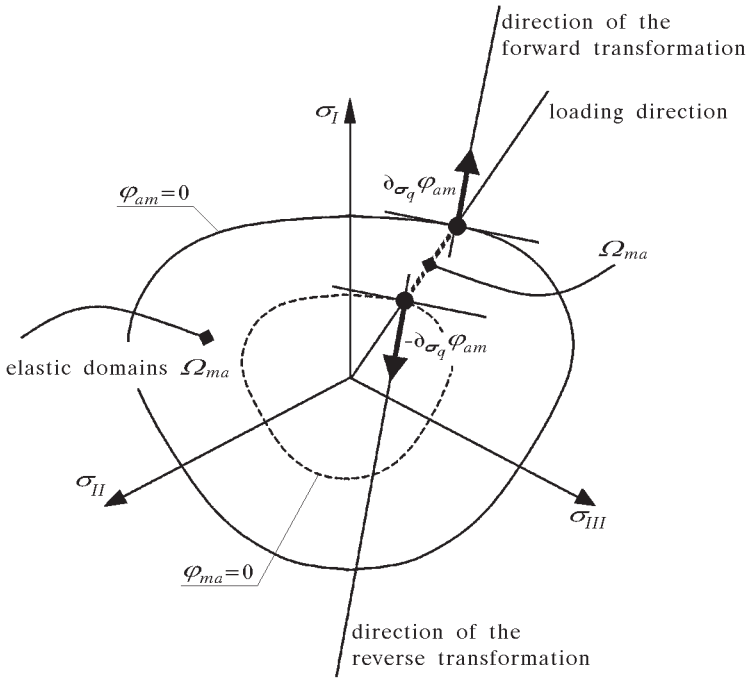


Fig. 3. Yield functions and transformation directions for each phase transition. Proportional loading case

If the forward transformation is interrupted, when unloading, the reverse transformation ( $a \leftarrow m$ ) can not occur in any direction, i.e.  $D_{ma}$  (3.4) is

not a full cone, since the phase transition strains must be recovered during the reverse transformation. From Eq. (3.11),  $D_{ma}[(\dot{\mathbf{d}}_q^{tr}, \dot{z}); (z, T)] \equiv D_{ma}[\dot{z}; (z, T)]$ . The simplest positively homogenous dissipation function of order one for the reverse transformation can then be chosen such as:

— for the forward transformation,  $\Pi_{am}(z, T) > 0$

$$D_{am}[\dot{z}; (z, T)] = \Pi_{am}(z, T)\dot{z} \tag{3.12}$$

— for the reverse transformation,  $\Pi_{ma}(z, T) < 0$

$$D_{ma}[\dot{z}; (z, T)] = \Pi_{ma}(z, T)\dot{z} \tag{3.13}$$

In this case, the normality rule  $\dot{z} = -\dot{\lambda}_{ma}\partial_{\Pi}\phi_{ma}$  with (Boubakar and Lexcellent, 2002)

$$\phi_{ma} = \Pi - \Pi_{ma}(z, T) \geq 0 \tag{3.14}$$

$$\Pi = \gamma_{\Sigma}(\partial_{\sigma_q}\Sigma)^{\top}\sigma_q + \rho\pi_0 - \rho\partial_z\psi^{di}$$

allows to build a unique yield function for the reverse transformations in the stress space, considering proportional loading-unloading paths (Fig. 3). Thus

$$\varphi_{ma} = (\partial_{\sigma_q}\Sigma)^{\top}\sigma_q - \Sigma_{ma}(z, T) \geq 0 \tag{3.15}$$

$$\gamma_{\Sigma}\Sigma_{ma} = -\rho\pi_0 + \rho\partial_z\psi^{di}(z, T) + \Pi_{ma}(z, T)$$

Within the context of a phenomenological approach, the threshold stress  $\Sigma_{ma}$  is defined from a uniaxial test (Boubakar and Lexcellent, 2002).

Following the generalized standard theory of materials, the direction of the reverse transformation for a given stress state must be normal at the corresponding point in the stress space to a convex domain  $\Omega_{\kappa}$  containing  $\Omega_{ma} = \{\Pi/\Pi - \Pi_{ma} \geq 0\}$  and turned towards the outside of this domain, i.e. a convex constraint domain is necessary to assure a global minimum for the intrinsic dissipation. The use of the maximum dissipation principle in order to derive the evolution laws giving  $\dot{\mathbf{d}}_q^{tr}$  and  $\dot{z}$  needs the definition of a potential function  $\kappa(\sigma_q, R)$  such that

$$\begin{aligned} \kappa(\sigma_q, R) &> 0 \quad \text{when} \quad \Pi - \Pi_{ma} > 0 \\ \kappa(\sigma_q, R) &= 0 \quad \text{when} \quad \Pi - \Pi_{ma} = 0 \end{aligned} \tag{3.16}$$

Since for proportional loading

$$\partial_{\sigma_q}\Sigma = \frac{\dot{\mathbf{d}}_q^{tr}}{\|\dot{\mathbf{d}}_q^{tr}\|} = \frac{\mathbf{d}_q^{tr}}{\|\mathbf{d}_q^{tr}\|} \tag{3.17}$$

the following function can be introduced

$$\kappa(\boldsymbol{\sigma}_q, R) = \frac{(\mathbf{d}_q^{tr})^\top}{\|\mathbf{d}_q^{tr}\|} \boldsymbol{\sigma}_q - \Sigma_{ma}(R) \geq 0 \quad \Sigma_{ma}(R) \equiv \Sigma_{ma}(z, T) \quad (3.18)$$

and then finally

$$\dot{\mathbf{d}}_q^{tr} = -\dot{\lambda}_{ma} \partial_{\boldsymbol{\sigma}_q} \kappa = -\dot{\lambda}_{ma} \frac{\mathbf{d}_q^{tr}}{\|\mathbf{d}_q^{tr}\|} \quad \dot{z} = \dot{\lambda}_{ma} \partial_R \kappa \quad (3.19)$$

$\dot{\lambda}_{ma} > 0$  is given by the consistency condition  $\dot{\varphi}_{ma} = 0$ .

#### 4. Application to the RLT models family

The previous sections presented a plasticity-type phenomenological modeling of the SMA superelasticity. Generalizing the main proposed approaches up to date, it enables to take into account different response configurations (Fig. 4) by defining suitable hardening laws, in absence of a good knowledge about the nucleation and the growth of martensite into austenite (Boubakar *et al.*, 2002). As shown in Boubakar *et al.* (2002), in the case of small strain hypothesis, the definition of a history-variable set allows to take into account a strong history-dependence of the behaviour.

Defining a relatively simple interaction energy  $\psi^{di}$ , the RLT models family allows to account quite well for the transformation configurations presented in the Fig. 4a where the place of the internal loops transition is located along a diagonal line. Concerning the choice of  $\psi^{di}$ , the simplest function  $z(1-z)$  such as  $\psi^{di} = 0$  for  $z = 0$  (pure austenite) and  $z = 1$  (pure martensite), has been introduced by Müller (1989, 1991), Huo and Müller (1993). Different features of these models can be specified within the proposed approach in Table 1.

#### 5. Parametric identification

Most of the models developed for the SMA superelasticity are based on a small perturbation formalism and their parameters are identified within this hypothesis. Thus, the RLT model parameters are identified directly from a pure tension test (Bouvet *et al.*, 2000). However, in the case of a finite strains analysis, the use of such parameters introduces errors. Willing to exploit the

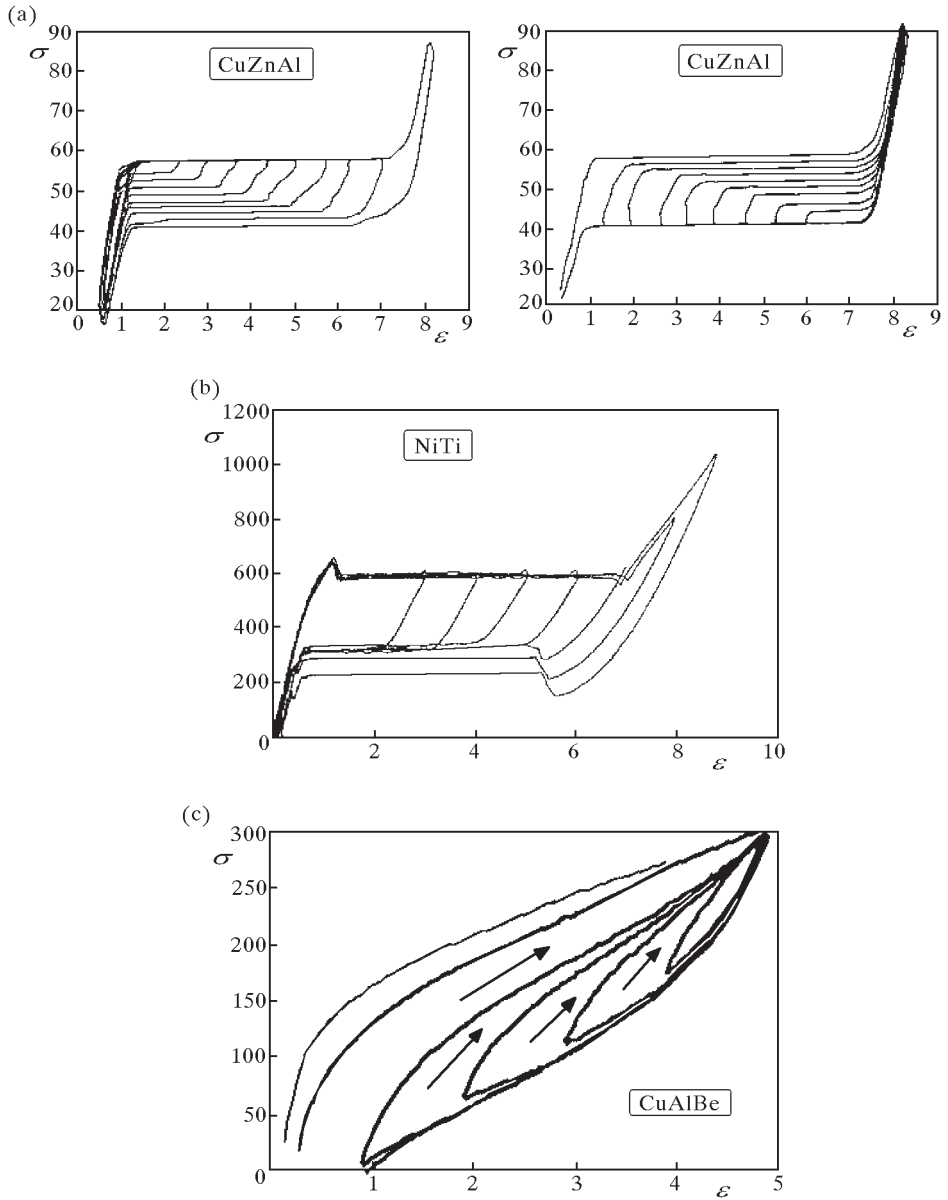


Fig. 4. Shape memory alloys superelastic responses: (a) CuZnAl (Huo and Müller, 1993), (b) NiTi (Lexcelent and Tobushi, 1995) and (c) CuAlBe (Bouvet, 2001)

**Table 1.** RLT model characteristics

<ul style="list-style-type: none"> <li>• Specific coherency energy</li> </ul> $\psi^{di}(z, T) = z(1 - z)\phi_{it}(T)$ <p>with <math>\phi_{it}(T) = u_0 - Ts_0</math>, <math>u_0</math> internal energy and <math>s_0</math> entropy <li>• State law</li> <math display="block">\boldsymbol{\sigma}_q = \rho \frac{\partial \psi^{el}}{\partial \boldsymbol{\varepsilon}_q^e} = \mathbf{C}^e \boldsymbol{\varepsilon}_q^e \quad \dot{\boldsymbol{\sigma}}_q = \mathbf{C}^e \dot{\boldsymbol{\varepsilon}}_q^e</math> <p><math>\mathbf{C}^e</math> elastic stiffness tensor</p> <li>• Forward transformation</li> <math display="block">\phi_{am} = \gamma_\Sigma \varphi_{am} = \Pi - \Pi_{am}(z, T) \leq 0 \quad \text{where} \quad \Pi_{am}(z, T) = k_1(z)</math> <ul style="list-style-type: none"> <li>• Reverse transformation</li> </ul> <math display="block">\phi_{ma} = \gamma_\Sigma \varphi_{ma} = \Pi - \Pi_{ma}(z, T) \geq 0 \quad \text{where} \quad \Pi_{ma}(z, T) = k_2(z)</math> <ul style="list-style-type: none"> <li>• Thermodynamic force</li> </ul> <math display="block">\Pi = \gamma_\Sigma (\partial_{\boldsymbol{\sigma}_q} \Sigma)^\top \boldsymbol{\sigma}_q + \rho \pi_0(T) - \rho(1 - 2z)\phi_{it}(T)</math> <ul style="list-style-type: none"> <li>• Transformation kinetics</li> </ul> <math display="block">k_1(z) = 2\phi_{it}(M_S^0)z + \frac{s_0 - \Delta s_0 - 2s_0z}{a_1} \ln(1 - z)</math> <math display="block">k_2(z) = -2\phi_{it}(A_S^0)(1 - z) + \frac{s_0 + \Delta s_0 - 2s_0(1 - z)}{a_2} \ln(z)</math> <p><math>M_S^0</math> is the forward transformation start temperature at stress free state; <math>A_S^0</math> is the reverse transformation start temperature at stress free state</p> <ul style="list-style-type: none"> <li>• Equivalent stress</li> </ul> <math display="block">(\boldsymbol{\sigma}_q)_{eq} = \overline{\boldsymbol{\sigma}}_q f(y_{\boldsymbol{\sigma}_q}) \quad \text{where} \quad f(y_{\boldsymbol{\sigma}_q}) = 1 + ay_{\boldsymbol{\sigma}_q}</math> <math display="block">\overline{\boldsymbol{\sigma}}_q = \sqrt{\frac{3}{2} dev(\boldsymbol{\sigma}_q) : dev(\boldsymbol{\sigma}_q)} \quad y_{\boldsymbol{\sigma}_q} = \frac{27 \det(dev(\boldsymbol{\sigma}_q))}{2 \overline{\boldsymbol{\sigma}}_q^3}</math> <p><math>a</math> is the material parameter characterizing the tension-compression dissymmetry</p> </p>
--

identification method perfected within the small strain context, the triaxial nature of the tension test involves a logarithmic cumulated tensorial deformation measure. This measure can be used in order to avoid the finite strain parameters reidentification. Consequently, a part of these parameters can be deduced from the one obtained for the small strain hypothesis using the following approach.

$\gamma$  representing the maximum transformation strain in tension, the logarithmic cumulated tensorial deformation measure leads directly to a relation connecting  $\gamma_{SP}$  to  $\gamma_{FS}$  ( $FS$  and  $SP$  denoting respectively Finite Strains and Small Perturbations)

$$\gamma_{FS} = \ln(1 + \gamma_{SP}) \quad (5.1)$$

Besides, although the transformation temperatures do not change whatever the approach used is (what means that the transformation start stresses do not change either), the other parameters introduced previously do depend on the same approach (Bouvet *et al.*, 2000)

$$\begin{aligned} (\Delta u_0)_{FS} &= \frac{\gamma_{FS}}{\gamma_{SP}} (\Delta u_0)_{SP} & \text{and} & & (u_0)_{FS} &= \frac{\gamma_{FS}}{\gamma_{SP}} (u_0)_{SP} \\ (\Delta s_0)_{FS} &= \frac{\gamma_{FS}}{\gamma_{SP}} (\Delta s_0)_{SP} & \text{and} & & (s_0)_{FS} &= \frac{\gamma_{FS}}{\gamma_{SP}} (s_0)_{SP} \end{aligned} \quad (5.2)$$

$\Delta u_0$  and  $\Delta s_0$  representing the internal energy and the entropy variation, respectively.

## 6. Applications

The RLT thermomechanical behaviour evoked mentioned has been implemented in the finite element code CASTEM 2000® in a spatial shell context. The model numerical integration has been validated by performing a set of different tests (Bouvet *et al.*, 2001; Boubakar and Vieille, 2002).

### 6.1. Tension-compression test

In order to bring out the tension-compression asymmetry behaviour, tests have been performed considering the experimental results given by Org as and Favier (1996). These tests have been made on NiTi samples whose material parameters are given in Table 2. The numerical simulation and the experimental points coincide quite well (Fig. 5).

**Table 2.** Tension/compression asymmetry – NiTi material parameters

$E$ [GPa]	$\nu$	$\rho$ [kg/m <sup>3</sup> ]	$\gamma_\Sigma$	$a_1$	$a_2$	$a$	$\Delta s_0$ [J/(kg·K)]	$s_0$ [J/(kg·K)]	$M_s^0$ [K]	$A_s^0$ [K]
55	0.29	6500	0.055	0.5	0.2	0.189	75	0	280	300

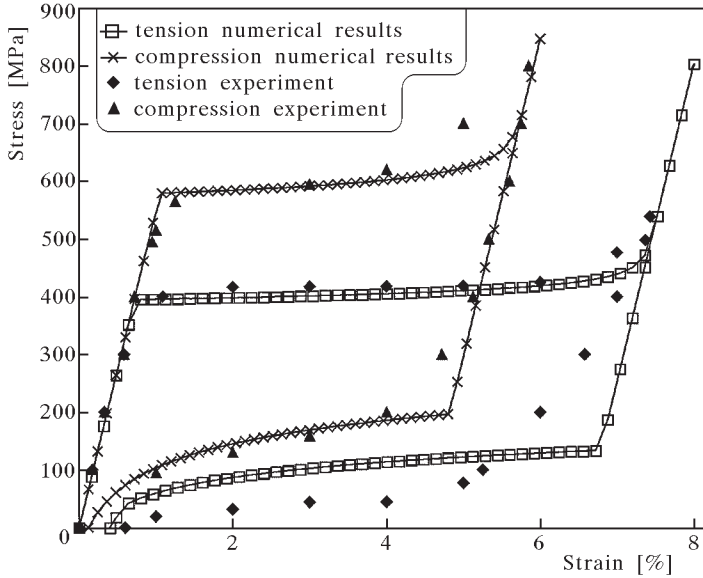


Fig. 5. Asymmetry effect between tension-compression

## 6.2. Partial loading or unloading

Indeed, considering more complex tests, the stress distribution in the structure is not uniform, that is why the direct and reverse transformations outset differs from one structure element to another. Whatever the case is, partial loading or unloading, the unstable balance line is the line where direct and inverse transformations start (Fig. 6). The material used for this test is a NiTi whose properties are given in Table 3 (Bouvet *et al.*, 2000). The numerical simulation and the experimental points coincide quite well for the external loops.

**Table 3.** Internal loops – NiTi material parameters

$E$ [GPa]	$\nu$	$\rho$ [kg/m <sup>3</sup> ]	$\gamma_\Sigma$	$a_1$	$a_2$	$a$	$\Delta s_0$ [J/(kg·K)]	$s_0$ [J/(kg·K)]	$M_s^0$ [K]	$A_s^0$ [K]
52	0.3	6700	0.05	5	5	0.2	50	0	200	284

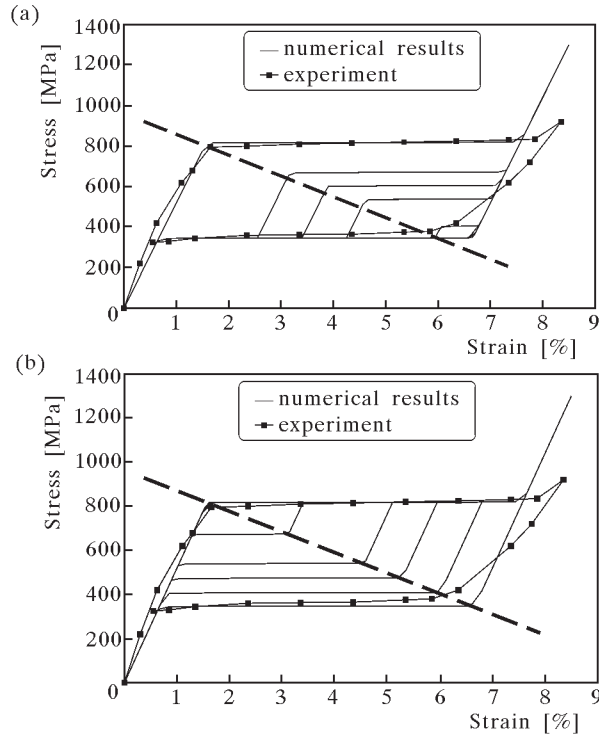


Fig. 6. (a) Partial loading; (b) partial unloading

### 6.3. Bulging test

A circular plate embedded around its circumference is submitted to a hydrostatic pressure uniformly distributed on its surface. Meshing, geometry and deformed shape are shown in Fig. 7. The material used for this test is CuZnAl whose parameters are presented in Table 4 (Rogueda, 1993). In Fig. 8 is presented the RLT model simulation for two thin films. Besides, the elastic finite strains simulations are compared with the analytical results obtained by using the Beams and Lin equations established for this example (BBeams, 1959; Lin, 1990).

**Table 4.** Bulging test – CuZnAl material parameters

$E$ [GPa]	$\nu$	$\rho$ [kg/m <sup>3</sup> ]	$\gamma_{\Sigma}$	$a_1$	$a_2$	$a$	$\Delta s_0$ [J/(kg·K)]	$s_0$ [J/(kg·K)]	$M_s^0$ [K]	$A_s^0$ [K]
58.6	0.2	8500	0.0358	0.05	0.5	0.142	22.46	4.06	282	295

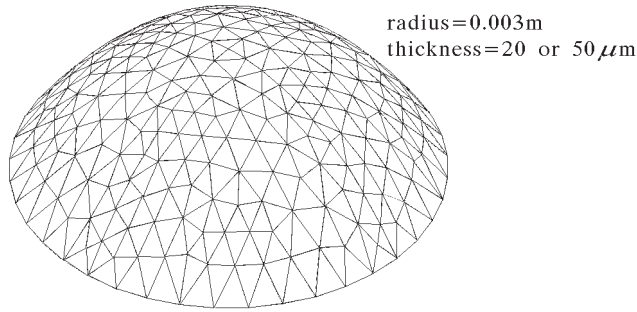


Fig. 7. Bulging test – deformed shape and dimensions

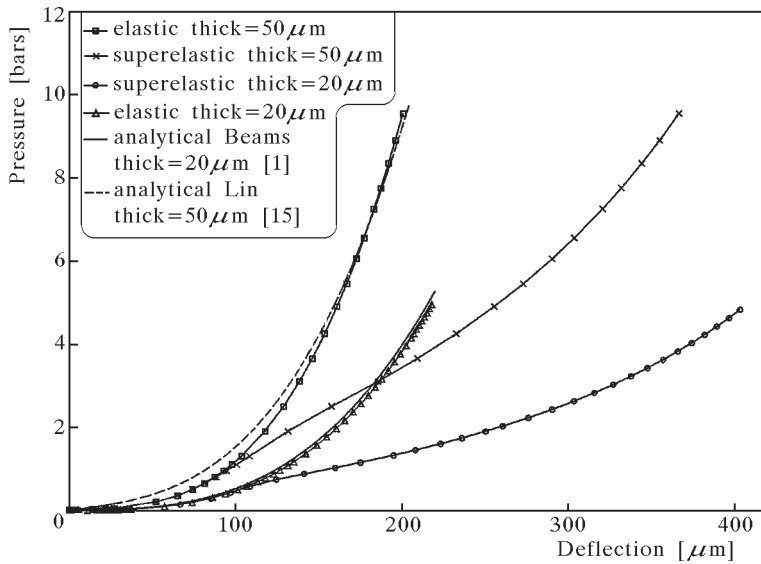


Fig. 8. Elastic and superelastic bulging test modelling

## 7. Conclusion

A non-material rotating frame formulation is proposed for the SMA superelastic finite strains calculation. It assumes that the alloy elastic behaviour is independent of the phase state. This approach takes place in the irreversible processes thermodynamics framework and assumes the behaviour to be independent from the deformation rate. It presents a formalism close to small perturbations. A numerical scheme in two stages has been adopted, consisting in an elastic prediction followed possibly by a superelastic correction (Bouvet

*et al.*, 2001). The numerical results obtained for a set of different tests allow to validate the SMA superelastic effect numerical integration in the particular case of the RLT model and using the shell finite elements. However, additional tests are necessary to confirm the proposed approach. It is the purpose of a running work involving a set of tests under non-proportional loadings. Indeed, the proposed modelling can be easily extended to that kind of loading.

## References

1. BEAMS J.W., 1959, *Structure and properties of thin films*, Eds. C.A. Neugebauer, J. Wiley and Sons, New York
2. BOUBAKAR M.L., 1994, Contribution à la simulation numérique de l'emboutissage des tôles. Prise en compte du comportement élastoplastique anisotrope, PhD Thesis, Franche-Comté University, Besançon, France
3. BOUBAKAR M.L., BOUVET C., HERZOG H., LEXCELLENT C., 2002, A general investigation of shape memory alloys thermomechanical behaviour modelling, submitted for publication
4. BOUBAKAR M.L., LEXCELLENT C., 2002, Some tools for modelling shape memory alloys. Thermomechanical behaviour and some efficient use, *Third World Conference on Structural Control*, Como
5. BOUBAKAR M.L., VIEILLE B., 2002, Superelastic Shell structures modelling. Part I: Element formulation, submitted for publication
6. BOUVET C., 2001, De l'uniaxial au multiaxial: comportement pseudoélastique des alliages à mémoire de forme, PhD Thesis, Franche-Comté University, Besançon, France
7. BOUVET C., BOUBAKAR M.L., LEXCELLENT C., 2000, Two normal dissipative processes for thermomechanical modelling of shape memory alloys, *IASS – IACM Fourth International Colloquium on Computations of Shell and Spatial Structures*, Chania, Greece
8. BOUVET C., BOUBAKAR M.L., LEXCELLENT C., 2001, Tension-compression asymmetry effect on the numerical modelling of pseudo-elastic shape memory alloys, *2nd Conference on Computational Mechanics*, Cracow
9. COSSERAT E., COSSERAT F., 1909, *Théorie des corps déformables*, Hermann, Paris
10. ECKART C., 1948, The thermodynamics of irreversible processes: IV. The theory of elasticity and anelasticity, *Physical Review*, **72**, 373

11. GILORMINI P., ROUDIER P., ROUGÉE P., 1993, Les déformations cumulées tensorielles, *Study for the Académie des Sciences*, **316**, Serie 2, 1499-1504
12. HALPHEN B., NGUYEN Q.S., 1975, Sur les matériaux standards généralisés, *J. de Mécanique*, **14**, 1, 39-63
13. HUO Y., MÜLLER I., 1993, Nonequilibrium thermodynamics of pseudoelasticity, *Continuum Mech. Thermodyn.*, **5**, 163-204
14. LEXCELLENT C., TOBUSHI H., 1995, Internal loops in pseudoelastic behaviour of Ti-Ni shape memory alloys: Experiment and modelling, *Meccanica*, **30**, 459-466
15. LIN P., 1990, In situ measurement of mechanical properties of multilayer-coatings, PhD Thesis, M.I.T., Boston, USA
16. MANDEL J., 1971, Plasticité et Viscoplasticité, *Cours CISM 97*, Udine-Springer, New York
17. MÜLLER I., 1989, On the size of the hysteresis in pseudo-elasticity, *Continuum Mech. Thermodyn.*, **1**, 125-142
18. MÜLLER I., XU H., 1991, On the pseudoelastic hysteresis, *Acta. Meta. Mater.*, **39**, 263-271
19. ORGÉAS L., FAVIER D., 1996, Non-symmetric tension-compression behaviour of NiTi alloy, *Journal of Physics IV*, **8**, 605-610
20. ROGUEDA C., 1993, Modélisation thermodynamique du comportement pseudoélastique des alliages à mémoire de forme, PhD Thesis, Franche-Comté University, Besançon, France

### **Sformułowanie problemu niestowarzyszonej supersprężystości w obrotowym układzie współrzędnych**

#### Streszczenie

W pracy przedstawiono metodę przewidywania i opisu stanu skończonych supersprężystych odkształceń określających zachowanie się stopów z pamięcią kształtu. Metodę oparto na reprezentacji kinematycznej stanu otrzymanej za pomocą wektorów kierunkowych. Metoda ta, jako spójna dla materiałów izotropowych i anizotropowych, umożliwiła wnioskowanie wprost z formalizmu techniki perturbacyjnej bazującej na małym parametrze. W szczególności, zaproponowano ogólne podejście do opisu supersprężystego zachowania się stopów z pamięcią kształtu poddanych proporcjonalnym obciążeniom przestrzennym.

*Manuscript received December 12, 2002; accepted for print March 5, 2003*